Nonlinear spatio-temporal filter to reduce crosstalk in bipolar electromyogram

Nonlinear spatio-temporal filter to reduce crosstalk in bipolar electromyogram

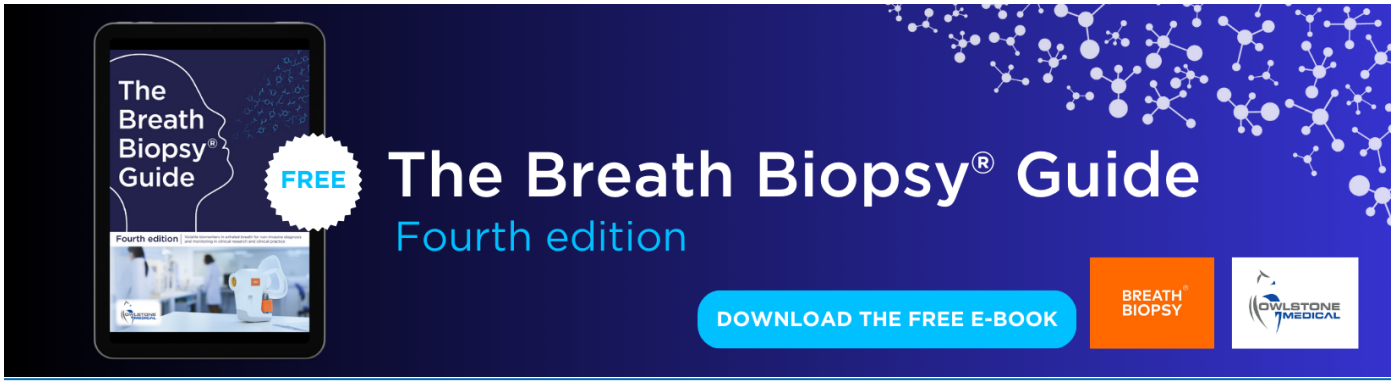

Journal of Neural Engineering

PAPER

Nonlinear spatio-temporal filter to reduce crosstalk in bipolar electromyogram

Luca Mesin

Mathematical Biology and Physiology, Department of Electronics and Telecommunications, Politecnico di Torino, Corso Duca degli Abruzzi 24, Turin, Italy

E-mail: luca.mesin@polito.it

Keywords: surface EMG, crosstalk, spatial filter

OPEN ACCESS

RECEIVED
14 August 2023

REVISED
6 January 2024

ACCEPTED FOR PUBLICATION
26 January 2024

PUBLISHED
9 February 2024

Abstract

Objective. The wide detection volume of surface electromyogram (EMG) makes it prone to crosstalk, i.e. the signal from other muscles than the target one. Removing this perturbation from bipolar recordings is an important open problem for many applications. *Approach.* An innovative nonlinear spatio-temporal filter is developed to estimate the EMG generated by the target muscle by processing noisy signals from two bipolar channels, placed over the target and the crosstalk muscle, respectively. The filter is trained on some calibration data and then can be applied on new signals. Tests are provided in simulations (considering different thicknesses of the subcutaneous tissue, inter-electrode distances, locations of the EMG channels, force levels) and experiments (from pronator teres and flexor carpi radialis of 8 healthy subjects). *Main results.* The proposed filter allows to reduce the effect of crosstalk in all investigated conditions, with a statistically significant reduction of its root mean squared of about 20%, both in simulated and experimental data. Its performances are also superior to those of a blind source separation method applied to the same data. *Significance.* The proposed filter is simple to be applied and feasible in applications in which single bipolar channels are placed over the muscles of interest. It can be useful in many fields, such as in gait analysis, tests of myoelectric fatigue, rehabilitation with EMG biofeedback, clinical studies, prosthesis control.

Abbreviations

ANOVA	Analysis of variance
BMI	Body Mass Index
BSS	Blind source separation
CoV	Coefficient of variation
EMG	Electromyogram
FCR	Flexor carpi radialis
IED	Inter-electrode distance
MDF	Median frequency
MNF	Mean frequency
MU	Motor unit
MVC	Maximum voluntary contraction
NLSTF	Nonlinear spatio-temporal filter
OSTF	Optimal spatio-temporal filter
PSD	Power spectral density
PT	Pronator teres
RMS	Root mean squared
SD	Single differential
SNR	Signal-to-noise ratio
SOBI	Second-Order Blind Identification

1. Introduction

Surface EMG is the signal recorded by electrodes placed on the skin and reflecting the bioelectric command inducing the contraction of a muscle [1]. The electrodes have a large detection volume [2, 3], so that they can record also the contribution from other muscles than the target one of interest [4, 5]. This undesired contribution, called crosstalk [6], is still an open problem in surface EMG. It is difficult to quantify and to remove and may affect different applications, as gait analysis [7], coordination [8] and control of myoelectric prosthesis [9–11].

Crosstalk was studied both using simulated [12–16] and experimental data [17–21]. Many results documented the difficulty of quantifying and removing crosstalk: cross-correlation of EMGs recorded over target and crosstalk muscles is not effective to measure the signal quality [22]; spatial filters have

different selectivity depending on the specific volume conductor [12]; simple temporal filters do not reduce it [23].

A common strategy to attenuate crosstalk is through appropriate electrode positioning [24] and the use of spatial filters [17, 19]. These filters reduce non propagating components [25], which provide the main contribution to crosstalk [26]. However, their effect depends on many factors (type/dimension of electrodes used, physical/geometrical properties of the tissues and anatomy of the subject) [12–16] and a small detection volume is explored, posing a problem of representativeness of the recorded information [27].

Advanced strategies have also been explored, e.g. decomposition algorithms [28, 29] and inverse methods [26, 30]. However, these processing algorithms are complicated and require a high-density detection. This is uncomfortable to use in many applications (e.g. ergonomics [31], sport science [32], gait analysis [33] and clinics [34]) where the set-up of the experiment should be fast, the detection has to be stable and the acquisition system must not hinder the movement.

An alternative approach is the OSTF [35, 36], which is adapted to the specific conditions (needing a preliminary training on selective data from target and crosstalk muscles) and can be applied in real-time. It requires simple recording systems (e.g. a few EMG channels over the target and the crosstalk muscles) and showed lower sensitivity to crosstalk than traditional spatial filters [36] and advanced BSS approaches [37]. However, the output of the filter is not easy to be interpreted. In fact, the motor unit (MU) action potential (MUAP) waveforms are in general different from those of well-known filters (e.g. the typical biphasic waveforms recorded by a bipolar filter). Moreover, the PSD can present dips and a bandwidth which is different from that of data usually recorded using simple spatial filters. In fact, OSTF performs both a spatial and a temporal filter, changing the typical distribution of sinusoidal components shown in the PSD of surface EMG. Finally, the output of the OSTF can change significantly whether applied to different subjects, experimental sessions of the same subject, or during different motor tasks (e.g. requiring different joint angles). Therefore, the adaptation of the method to specific conditions, depending mainly on electrodes locations and physical properties of the volume conductor, makes tricky a comparison among different acquisitions.

Thus, it would be much simpler to interpret the data provided by an algorithm giving an estimation of the classical bipolar EMG from the target muscle after removing the contribution of crosstalk. This paper addresses this problem. A possible solution could be using a BSS method: such an approach was proposed to estimate the contributions of two nearby muscles (removing crosstalk from each other) by assuming that recorded signals are linear instantaneous mixtures of decorrelated sources [20]. The method was applied offline on the entire signals, but the de-mixing matrix could be estimated on a portion of data and then kept fixed and applied online on new data.

The de-mixing matrix is a set of spatial filters adapted to the subject to remove crosstalk from each signal. A generalization of using spatial filters is obtained by including also delayed samples (thus, applying a spatio-temporal filter) and making a non-linear processing of the data. In this way, a NLSTF is obtained. This paper explores this approach, introducing an innovative NLSTF to reduce the amount of crosstalk from single differential (SD) data, providing as output an estimation of the bipolar EMG from the target muscle. This method is compared to a BSS approach, trained and tested on the same data.

2. Methods

2.1. Design of the optimal filter

An optimal filter is designed to provide as output the signal from the target muscle, giving as input the data corrupted by crosstalk recorded over the target and the cross-talk muscles. The filter is built by training on SD signals recorded over the target and the crosstalk muscles during selective contractions. Specifically, assume that we consider only 2 muscles, i.e. a target and a single crosstalk muscle. Two SD channels are placed, one over each muscle. We indicate by $x_{ij}(t)$ the signal recorded over the muscle i and produced by the muscle j, where i (j) is equal to 1 or 2 for the target and crosstalk muscle, respectively. These signals are summed to generate data corrupted by crosstalk $x_i(t) = x_{i1}(t) + x_{i2}(t)$. Using the information contained in $x_1(t)$ and $x_2(t)$ (i.e. the signals recorded respectively over the target and crosstalk muscles and produced by their co-contraction), the objective is to estimate $y(t) = x_{11}(t)$ (i.e. the SD signal recorded over the target muscle and produced only by it).

An approach similar to that proposed in [38] is used, to obtain a NLSTF.

A linear least squared problem is defined with respect to the weights of the filter, using present and past samples (up to N lags) of the 2 SD channels. This way, both spatial and temporal filters are defined. Also quadratic terms have been included, i.e. instantaneous cross-correlations and energies (preserving information on the sign, i.e. $-x^2(t)$ was used for samples for which $x(t) < 0$). Thus, a nonlinear processing of the input data was performed, but still solving a linear problem for the filter weights.

In detail, the desired output was fit by the following linear model

$$y = XW + r \tag{1}$$

where W is the vector of filter weights, r the residual error and the matrix X includes the predictors, i.e. the 2 SD signals, their delayed versions up to N lags and the cross-product of all these terms. A general expression of X is

$$X=\begin{bmatrix} 1 & \cdots & \cdots & \cdots & \cdots & \cdots & \cdots & \cdots & \cdots & \cdots & \cdots \\ 1 & x_1(i) & x_1(i-1) & \cdots & x_2(i-N) & x_1^2(i) & \cdots & x_2^2(i-N) & \cdots & x_1(i-k)x_2(i-n) & \cdots \\ \vdots & \vdots & \vdots & \vdots & \vdots & \vdots & \vdots & \vdots & \vdots & \vdots & \vdots \\ 1 & x_1(S) & x_1(S-1) & \cdots & x_2(S-N) & x_1^2(S) & \cdots & x_2^2(S-N) & \cdots & x_1(S-k)x_2(S-n) & \cdots \end{bmatrix} \quad (2)$$

where the vector of 1s is used to account for a bias; N is the order of the temporal filter; S is the number of samples in the training set; i is a generic sample; k and n are general delays ($\leqslant N$); for brevity, the square symbol was used, but the sign was kept (thus, $x_i^2(j)$ was substituted by $sign(x_i^2(j))|x_i^2(j)|^2$).

The matrix X was decorrelated, by eigendecomposition of the correlation matrix X^TX, obtaining the eigenvectors matrix V, such that the new predictors $Y=XV$ were orthogonal. Then, the least absolute shrinkage and selection operator was used to estimate the filter weights in order to reduce the residual error and select the essential predictors, avoiding overfitting [39]. Specifically, the following functional was minimized with respect to the weights W

$$\|y-YW\|_2^2+\lambda\|W\|_1 \quad (3)$$

where λ is a regularization parameter balancing the squared residual (in estimating the crosstalk-free SD signal $y(t)$) and the L_1 norm of the weights, chosen minimizing the 10-fold cross-validation error.

The matrix of eigenvectors V and the optimal weights W should contain essential information on the volume conductor and on the detection system, allowing to compensate their influence in corrupting target data with crosstalk. Assuming that their effect is constant during the experiment, V and W are kept fixed and applied to test data.

2.2. Blind source separation

The NLSTF was compared to a method of BSS based on SOBI, introduced in [40] and then applied to crosstalk in surface EMG [20].

The method is based on the assumption that the recorded data are instantaneous linear mixtures of decorrelated sources [41]. The mixing matrix can be estimated in two steps [20]:

(i) whitening, which imposes that the sources are spatially decorrelated;
(ii) rotation, which assumes that the instantaneous cross-correlation of the sources is diagonal; it was implemented in the time–frequency domain, by joint diagonalization of matrices of spectra sampled at K time–frequency points (where K was chosen by a fine tuning on few data).

Once obtained the mixing matrix, SOBI provides a de-mixing matrix (by pseudo-inversion) that, applied to the recorded data, provides decorrelated sources which, eventually, approximate the signals from the two muscles.

SOBI was applied to our signals in a similar fashion as the NLSTF: specifically, the de-mixing matrix was trained on a portion of data (i.e. the same used for training the NLSTF) and then kept fixed and applied to test data. The source with largest correlation with the ideal target signal was selected, with amplitude optimally chosen to minimize the RMS error.

2.3. Simulated signals

The cylindrical model proposed in [42] was used to simulate single fibre action potentials (SFAP) from two muscles (figure 1). A 2D grid of square electrodes (surface 1 mm^2) with inter-electrode distance (IED) of 10 mm was used, with arrays of 3 electrodes placed aligned to the fibres. The average length of simulated muscle fibres was 10 cm, with a random uniform spread of tendon endings of 10 mm; the innervation zones (IZ) were located about in the middle of the fibres with random displacement in a range of variation of 10 mm (uniform distribution). Monopolar SFAPs were simulated, from which SD recordings with different detection points and IEDs were obtained. Fibre density was 20 mm^{-2}, which is about 10 times smaller than the physiological value (it is about the density of fibres of MUs [43]) and the same fibres were included in different MUs with superimposed territory (which introduces a small approximation error). MU sizes were exponentially distributed in the range 15–300 and 200 MUs were simulated for each muscle. Their locations were chosen randomly, with uniform distribution within the muscles, whose cross-sections are shown in figure 1(B). The fibres closest to the centre of a MU were selected to belong to it and MUAPs were generated summing the corresponding SFAPs. A Gaussian distribution with mean 4 m s^{-1} and standard deviation 0.3 m s^{-1} was assumed for the MU

conduction velocity (CV); a reduction of 20% was used to test the algorithm on data affected by peripheral fatigue. CV values were assigned according to the size principle [44].

Interference signals were simulated as in [43], with largest recruitment threshold equal to 60% of the MVC, mean firing rates (FR) with range 8–30 Hz (after MU recruitment, the mean FR increased linearly with force, with slope of 1 Hz per 1% MVC, with saturation at 30 Hz) and random (Gaussian) jitter with zero mean and standard deviation of 10% of the mean inter-spike interval. Force levels of 10%–100% MVC (10% step) were simulated.

2.3.1. Simulation tests

The algorithm for the estimation of the SD signal from the target muscle has been applied in different conditions. The following parameters were varied in different tests in simulation.

- Fatigue: test data were either equivalent to those used for training or affected by fatigue, inducing a 20% reduction of the CV of all MUs.
- Transverse distance: either 20 mm or 40 mm from the median line separating the two muscles.
- IED: 10 mm or 20 mm.
- Noise: white Gaussian noise was added to the simulated monopolar data before building the SD filter, with either 30 dB or 20 dB of SNR.
- Training was applied either to selective contractions or to data corrupted by a contraction of 5% MVC of the muscle assumed to be silent.
- A volume conductor with thickness of the fat layer of either 3 mm or 7 mm was used to generate the MUAPs.
- EMGs related to force levels of 10%–100% MVC (10% step) were generated for each muscle and summed with all possible combinations to simulate co-contractions.
- Five different distributions of MUs within the muscles were generated (to get different 'simulated subjects').

Thus, in total, the dataset of simulations on which the method was tested included 32 000 signals (i.e. either including or not fatigue, with 2 possible transverse distances, 2 IEDs, 2 noise levels, using for the training either selective contractions or not, 2 fat layer thicknesses, producing 10 force levels with the target muscle and 10 others with the crosstalk muscle, considering 5 subjects).

2.4. Experimental data

The experimental data used to test the algorithm are the same as in [36] (to which the reader can refer for details). In short, eight healthy volunteers participated in this study (six males; mean ± standard deviation: age 28.1 ± 7.5 yr, height 176.8 ± 7 cm, weight 71 ± 11.2 kg, BMI 22.4 ± 2.4). The experiments were conducted in accordance with the Declaration of Helsinki and with the approval of the Ethical Committee of University of Turin (approval number 510190).

Monopolar EMGs were recorded with reference electrode on the elbow, using the amplifier Quattrocento (OT Bioelettronica, Turin, Italy) during selective contractions of FCR and PT. The two muscles are close to each other (making relevant the issue of crosstalk) and are devoted to different movements, i.e. flexion and pronation, respectively. The dominant (right) forearm of each subject was placed in a support, to which a 'handle' was connected through two load cells (from which torque signals were amplified and sampled at 10 Hz using two ADCs with 24 bits resolution, controlled by an Arduino UNO board), one for each side, allowing to quantify the applied force and type of effort (i.e. either flexion or pronation). After skin cleaning, a grid of 13 rows and 5 columns of electrodes with 8 mm IED was placed so that ideally two columns were over the PT, two on the FCR and the central one in between. Surface EMGs were amplified, band-pass filtered (−3 dB bandwidth, 10–500 Hz), sampled at 2048 Hz and converted in digital form with a resolution of 16-bit. Data were finally sent to a workstation, for further processing with MATLAB (Inc. Natick, Massachusetts, USA, ver. 2023a). A visual feedback was provided to the subject, to help keeping approximately isotonic contractions at specific levels.

For each task (i.e. flexion and pronation), three MVCs were first measured (with 120 s rest between them) and the largest value was selected. Then, for each muscle, 20 s submaximal contractions of 10%–50% MVC (with 10% step) in random order were recorded with 60 s of rest between them, from which the central epochs of 10 s (considered as quite stationary) were selected for processing.

Bipolar data from the two muscles were obtained using electrodes from the external columns (in order to be sure to be over a single muscle). The same rows were used for the electrodes of the two channels, so that the detection systems were side-by-side. They were placed beyond the most distal IZ of the two muscles, considering two IEDs (8 mm and 24 mm, keeping the same detection point). A final test was also carried out by including a third detection channel from the central column, placed between the other two.

2.5. Test of performances

Data were combined to simulate the co-contraction of pairs of muscles, both when considering simulations and experimental signals. The first second of data was used for training, both in the tests with simulations and experimental EMG. The algorithms SOBI and NLSTF were trained to recover the crosstalk-free SD EMG of the target muscle from the combined signals recorded over the two muscles. Data of

crosstalk muscle were circularly shifted with 5 different translations to augment the training. Then, they were summed to the EMG of the target muscle to train the NLSTF; target and crosstalk signals were instead concatenated to train SOBI. The optimal number K of time–frequency points for the joint diagonalization step in SOBI algorithm was chosen by a fine tuning on a few tests: $K = 2000$ for simulations and $K = 600$ for experimental data.

Then, SOBI and NLSTF were applied for testing on the data not used for training. The performances of the algorithms were indicated in terms of the root mean squared (RMS) error of the residual when estimating the SD signal produced by the target muscle (in percentage with respect to the RMS of the correct SD signal from the target muscle). When the algorithms are not applied, the residual error is equal to the percentage RMS of the crosstalk signal recorded over the target muscle. This value was used as reference, to test the importance of processing the data.

Furthermore, the possibility of estimating classical amplitude and spectral indexes was investigated. The RMS of the signal was used as amplitude estimator (notice that the amplitude of the output of SOBI is not determined, so that the RMS amplitude was computed only for the ideal signal, the raw data and the EMG filtered by the NLSTF). Moreover, mean and median frequencies (MNF and MDF, respectively) were computed as spectral indexes. These amplitude and spectral parameters were estimated from the target signal (used as reference), the noisy data corrupted by crosstalk and the filtered EMG (obtained by applying either SOBI or NLSTF to the noisy data). The absolute errors of the RMS amplitude (in percentage with respect to the RMS of the target signal) and of the spectral indexes were computed, by comparing estimations from either the noisy or the filtered data with the reference.

Overall results of the performance indexes were computed. Then, the analysis was deepened for two of them: the RMS error (providing the accuracy in reconstructing the target signal) and the error in estimating MDF (indicating the possibility of getting accurate information on the spectral content of the target signal). In order to detect possible statistically significant differences, multifactorial ANOVAs were applied on the difference between these two performance indexes obtained by using data processed by the NLSTF and either the raw data or the output of SOBI. Specifically, for simulations, there were 8 factors (fatigue, transverse distances, IEDs, noise levels, selectivity of contractions, fat layer thickness, force levels of target and crosstalk muscles) and for experimental data 4 factors (muscle considered as target, IED, force levels of target and crosstalk muscles). ANOVA models with two-factor interactions were used.

Standard parametric tests were applied after transforming the data (i.e. RMS error and absolute error in MDF estimation). The classical Box-Cox transformation [45] did not provide satisfying results. Then, monotonic transformations of the data (preserving ranks) were chosen by solving optimization problems imposing that the residuals had distributions close to Gaussian and were homoscedastic across groups. The performances of the transformations were indicated in terms of the following parameters, measuring the goodness of fit of the hypotheses of the parametric ANOVA models (i.e. gaussianity and homoscedasticity of residues): L_1 difference between a Gaussian (with same mean and standard deviation as the corresponding sample estimations) and the probability density distribution of the residues (obtained by the kernel density estimation, using 100 points and normal kernel), skewness, kurtosis and CoV of their standard deviations across groups.

Finally, differences of distributions of performance indexes were also displayed after pooling with respect to factors (without transforming the data, but showing the differences of the original values).

3. Results

The simulation model is depicted in figure 1, indicating the volume conductor in figure 1(A) and the cross-section in 1(B). Monopolar signals from different electrodes were simulated, in order to be able to generate bipolar EMGs with different locations and IEDs. Some examples of interference signals are shown in figure 1(C): the same MU firings were used to generate EMGs recorded with bipolar channels with different locations and IEDs. As expected, the effect of crosstalk decreases when the detection is more selective (i.e. smaller IED) and located further away from the crosstalk muscle.

Figure 2 illustrates the experiments, indicating the two muscles under study in 2(A), the experimental protocol in 2(B) and some examples of data in 2(C) (considering bipolar channels with different locations and IEDs).

Examples of processing are shown in figure 3. Both simulated (panels 3(A) and (C)) and experimental data (3(B) and (D)) are considered, either in time (3(A) and (B)) or in frequency domain (3(C) and (D)). Data from target and crosstalk muscles were summed to generate a noisy signal, which was corrupted by crosstalk as in the case of a co-contraction. SOBI and NLSTF were then applied to the noisy data to estimate the signal from the target muscle. The contraction levels were selected for the simulated and experimental conditions to get similar contributions of crosstalk. The RMS errors for the estimation of the target signal using either SOBI or NLSTF are shown.

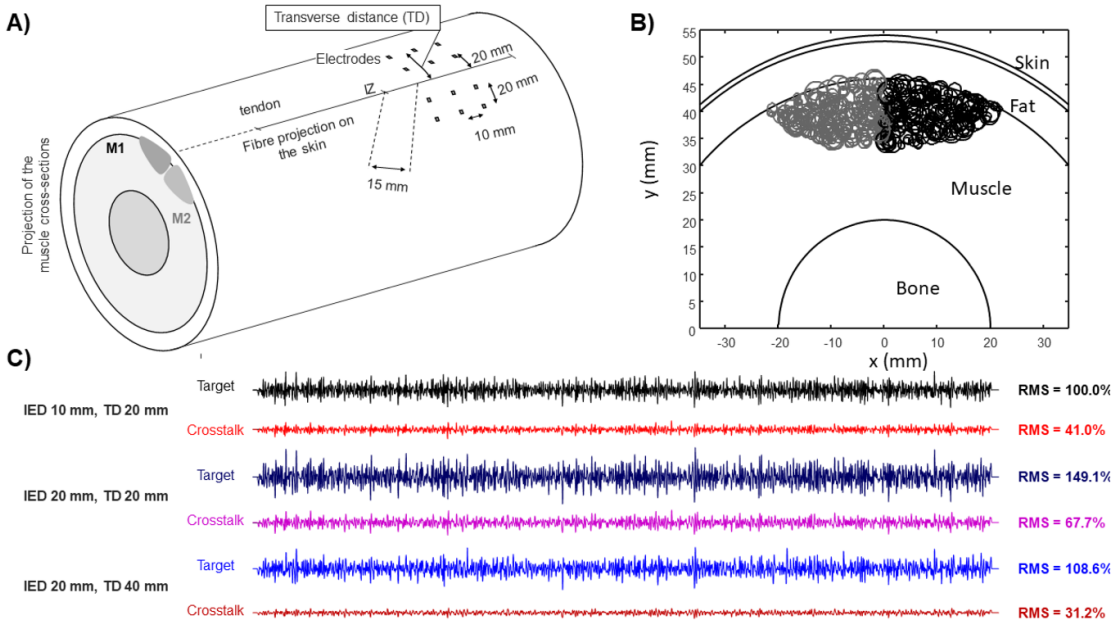

Figure 1. Generation model used for the simulation of surface EMGs. (A) Three dimensional view of the cylindrical volume conductor. Tissue thickness/conductivities are 1 mm/50 · 10^{-2} S m^{-1} for the skin, 3 or 7 mm/5 · 10^{-2} S m^{-1} for the fat, 20 mm (radius)/2 · 10^{-2} S m^{-1} for the bone, 26 mm for the muscle with longitudinal/transverse conductivity 50/10 · 10^{-2} S m^{-1}. The simulated electrode grid is also indicated: monopolar signals were simulated and then different electrodes were used to generate bipolar signals with different inter-electrode distances (IED) and detection points. (B) Cross-section of the volume conductor: centres and dimensions of MUs of a single simulated subject are indicated with circles with correct centre and cross-sectional area, for simplicity of representation. (C) Examples of single differential (SD) signals generated by a muscle (at 50% MVC) and recorded with different IEDs (volume conductor with 7 mm of fat thickness). The SD channels are placed in different locations: either over the contracted muscle or on the relaxed one, obtaining the target and crosstalk signal, respectively; the transverse distances (TD) from the mid-line separating the two muscles is either 20 or 40 mm.

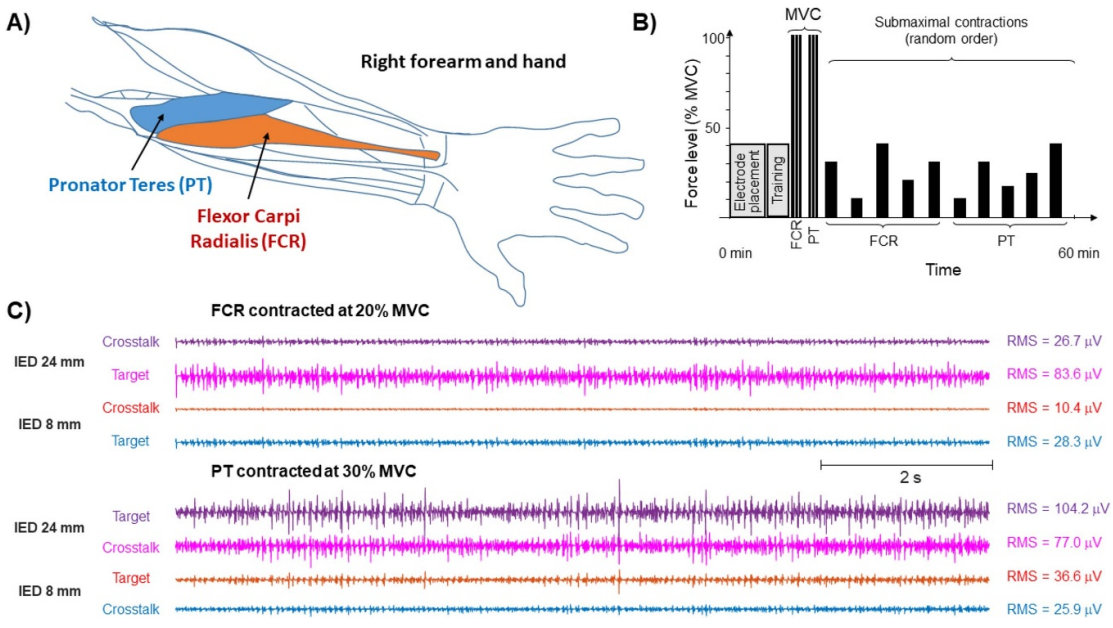

Figure 2. Example of real data and description of the experimental protocol. (A) Indication of the investigated muscles: Flexor Carpi Radialis (FCR) and Pronator Teres (PT). (B) Timings of the experimental protocol. (C) Examples of data from a subject. The two muscles are considered during selective contractions of different levels, using two single differential (SD) channels (placed over each muscle, at 16 mm from the mid-line separating them) with different IED.

The entire simulated and experimental datasets are now considered. Statistical effects of factors on simulations are first explored, using ANOVA tests applied on differences of performance indexes (RMS error and mistake in MDF estimation), obtained using NLSTF vs SOBI or NLSTF vs the original signals. Those data were transformed monotonically (as explained in the Methods section) to make the

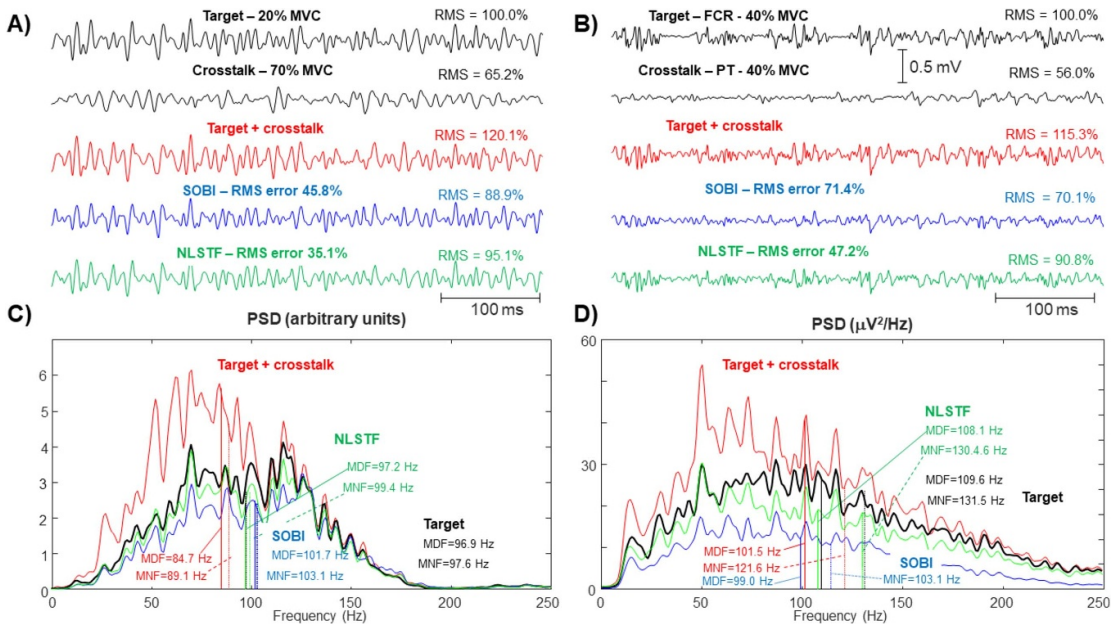

Figure 3. Examples of target, crosstalk, perturbed and filtered data (by either SOBI or NLSTF). (A) Simulated data (fat layer thickness 3 mm, IED = 20 mm, distance from the mid-line separating the two muscles equal to 20 mm). A portion of testing signal is shown out of a processed signal of 5 s (1 s of data was used for training SOBI and NLSTF). Five signals are shown: target, crosstalk, perturbed data (i.e. the sum of target and crosstalk signal recorded from the bipolar channel placed over the target muscle) and signals filtered by SOBI and NLSTF. The indication of the RMS amplitude (referred to that of the target signal) is shown for each signal. Moreover, the RMS of crosstalk is a measurement of error when using the raw data (which is the sum of the signals from the target and crosstalk muscle); the RMS errors of SOBI and NLSTF in estimating the target signal are also given, as a percentage of the RMS of the target signal. (B) Same as (A), but considering a portion of experimental data extracted from signals of duration 10 s, of which 1 s was used for training SOBI and NLSTF. Bipolar EMGs with IED = 24 mm are shown, in which the flexor carpi radialis (FCR) and the pronator teres (PT) are considered as target and crosstalk muscles, respectively. (C) Power spectral density (PSD) of the simulated signals shown in (A) (Welch method, with Tukey window with cosine fraction of 10%, duration 250 ms, overlap of 50% and zero padding to get apparent resolution of 1 Hz), with indication of the estimated spectral indexes. (D) Same as (C), but for the experimental signals shown in (B).

residual errors after linear fitting closer to Gaussian and homoscedastic. Table 1 provides some indexes measuring the fit of the hypotheses of parametric multifactorial ANOVA. The transformed data better fit the hypotheses than the original and those processed by the optimal Box-Cox transformation. ANOVA was applied on those transformed data. The list of factors and interaction terms showing statistically significant differences are reported in table 2. The single factors provided significant effects in most cases and also many interaction terms.

Figure 4 shows distributions of results (using violin plots [46]), obtained from the dataset of simulations. The focus is on the ability of SOBI and NLSTF to estimate the crosstalk-free bipolar signal from the target muscle. The percentage RMS error is shown in 4(A) and the absolute error in estimating MDF is reported in 4(B), after pooling data to indicate single effects of interest, regarding the volume conductor (i.e. fat layer thickness), the location of the detection point (in terms of the distance from the crosstalk muscle), the selectivity of the SD filter (related to the IED) and problems in the input signals (noise with different SNRs, not selective contractions for training, myoelectric fatigue in the test). In all conditions, NLSTF showed smaller average errors in estimating the target signal than SOBI and large improvements with respect to using raw data. Results follow our expectations: estimation errors increase when test data include myoelectric fatigue, crosstalk muscle is closer, IED is larger (i.e. SD filter is less selective), noise is larger and the fat layer is thicker (thus, diffusing more the crosstalk signal). The only unexpected result is a reduction of the estimation error of MDF when the training set is perturbed by using not selective contractions; this result is subverted when myoelectric fatigue is neglected (notice the significant interaction between fatigue and selectivity disclosed by ANOVA tests shown in table 2).

Considering the entire dataset, the following median errors were obtained when estimating the target SD signal using raw data, SOBI and NLSTF, respectively: 23.7%, 21.4% and 17.4% for the RMS error (median improvement with respect to using raw data of 4.4% and 5.9%, median percentage reduction 19.6% and 25.5% for SOBI and NLSTF, respectively); a marginal improvement in RMS amplitude estimation was obtained, with 2.57% of median error when using the NLSTF, instead of 2.58% for the raw data (the mean percentage error showed a larger decrease, from 5.9% with raw data to 4.6% using the output of NLSTF; notice that the amplitude of the output of SOBI is not defined and it was chosen in order to minimize the error in estimating the ideal crosstalk-free

Table 1. Simulated data: comparison of NLSTF and either raw data or SOBI. Different indexes are shown to characterize the deviations from hypotheses of ANOVA of residues of errors after linear fit (with interactions). Goodness of fit was measured as the integral of the absolute difference between the distribution of data and a Gaussian with mean and standard deviation equal to the sample estimates. Goodness of fit, skewness and kurtosis indicate the deviation from the hypothesis that the residues have Gaussian distribution. CoV(σ) indicates the coefficient of variation of the standard deviation of the residues across groups, as an indicator of the divergence from the hypothesis of homoscedasticity. In the case of Box-Cox transformation, λ is the optimal exponent.

	NLSTF—Raw					
	RMS error			Error in MDF estimation		
	Raw data	Box-Cox $\lambda = 3.86$	Monotone Transform	Raw data	Box-Cox $\lambda = 1.72$	Monotone Transform
Goodness of fit	1.38	1.43	0.10	1.52	0.18	0.09
Skewness	−1.52	0.88	0.02	1.29	4.24	0.26
Kurtosis	23.40	14.13	4.24	35.44	146.62	3.00
CoV(σ)	1.21	0.81	1.12	0.96	0.96	0.63
	NLSTF—SOBI					
	RMS error			Error in MDF estimation		
	Raw data	Box-Cox $\lambda = 4.86$	Monotone Transform	Raw data	Box-Cox $\lambda = 2.54$	Monotone Transform
Goodness of fit	1.23	1.01	0.04	1.44	1.00	0.05
Skewness	−1.32	0.46	0.02	−0.38	4.91	0.21
Kurtosis	14.31	22.04	3.01	18.75	220.86	2.94
CoV(σ)	1.42	0.96	0.54	1.06	1.00	0.53

Table 2. Simulated data. Statistically significant factors and interactions in the ANOVA model applied to error differences (i.e. error of NLSTF output minus that obtained either using raw data or signals provided by SOBI). Both RMS error and MDF estimation error are considered. Single terms indicate single factors with significant differences; couples of factors indicate interaction terms. Target muscle (M1) and crosstalk muscle (M2).

		Simulations—significant terms in ANOVA model ($p < 0.001$)
NLSTF—Raw	RMS error	All factors, fatigue-selectivity, fatigue-force M2, TD-fat, TD-force M1, TD-force M2, IED-fat, IED-force (M1 and M2), selectivity-force (M1 and M2), fat-force (M1 and M2), force M1-force M2
	MDF error	All factors except for noise level, fatigue-selectivity, fatigue-force (M1 and M2), TD-(All factors except for fatigue), IED-fat, IED-force (M1 and M2), selectivity-fat, selectivity-force M2, fat-force (M1 and M2), force M1-force M2
NLSTF—SOBI	RMS error	All factors except for selectivity, fatigue-IED, fatigue-fat, fatigue-selectivity, fatigue-force (M1 and M2), TD-selectivity, TD-force (M1 and M2), IED-noise level, IED-fat, IED-force M2, selectivity-force (M1 and M2), selectivity-fat, fat-force (M1 and M2), force M1-force M2
	MDF error	All factors except for noise level, fatigue-selectivity, fatigue-force (M1 and M2), TD-selectivity, TD-fat, TD-force (M1 and M2), IED-force M1, selectivity-force (M1 and M2), fat-force (M1 and M2), force M1-force M2

signal); 1.01 Hz, 1.13 Hz and 0.50 Hz for the error in estimating MDF (for NLSTF, median difference 0.34 Hz, median percentage reduction of the error equal to 46.1%; SOBI worsened MDF estimation); 0.81 Hz, 3.88 Hz and 0.69 Hz for the error in estimating MNF (for NLSTF, median difference 0.03 Hz, median percentage reduction 6.1%; SOBI worsened MNF estimation).

The beneficial effects of the investigated filters (SOBI and NLSTF) depend on the contraction levels of the two muscles. For example, pooling simulated conditions, when estimating the target SD signal using raw data, SOBI and NLSTF (respectively), the median RMS error decreased from about 88.6%, 61.0% and 55.7% to 15.2%, 15.8% and 11.7% when the force level of the target muscle increased from 10% to 100% MVC; on the other hand, it increased from about 7.1%, 15.6% and 6.8% to 36.5%, 26.7% and 24.3% when the force level of the crosstalk muscle increased from 10% to 100% MVC.

Notice that, considering the overall results, there are conditions in which crosstalk is either marginal or important, specifically when the force level of crosstalk is either larger or smaller (respectively) than that of the target. Obviously, the importance of using a filter (either SOBI or NLSTF) is more evident when the crosstalk perturbation is larger: considering only contractions in which the force level of the crosstalk muscle was equal or larger than that of the target, the median reductions of RMS error, RMS amplitude,

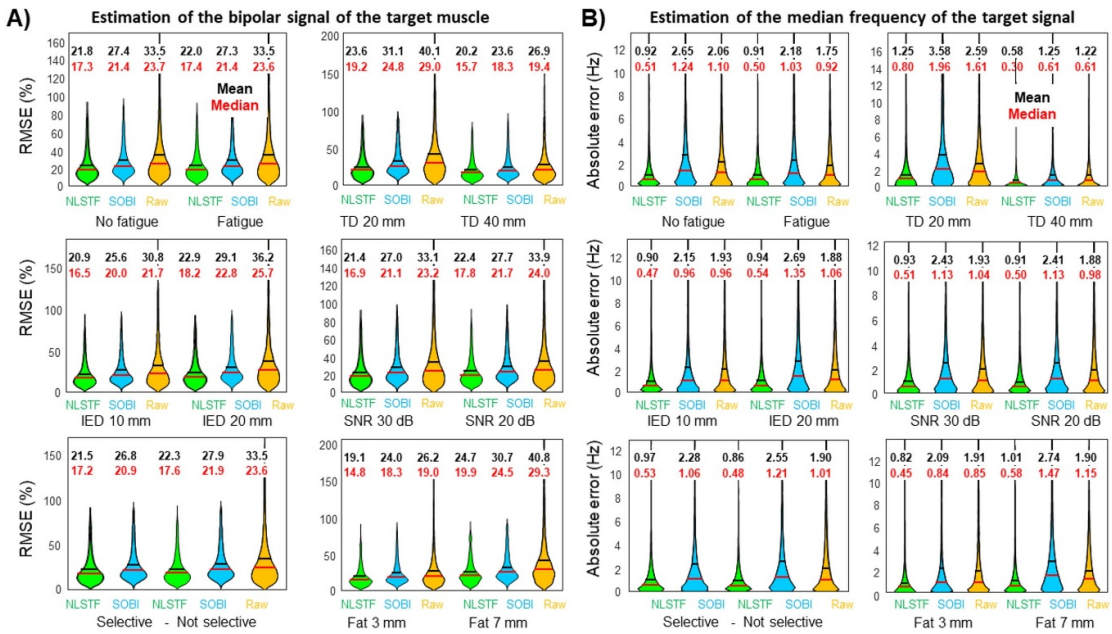

Figure 4. Summary of the processing of the simulation dataset, pooling the results to show the effect of different parameters of interest: test EMGs either affected by fatigue or not, transverse distance (TD) from the mid-line separating the two muscles either 20 mm or 40 mm, IED of 10 mm or 20 mm, SNR of the monopolar signals of 30 dB or 20 dB, contractions generating the training EMGs either selective or including crosstalk (with force level 5% MVC), volume conductor with fat layer thickness of 3 mm or 7 mm. Violin plots are shown with indication of median and mean of the distributions. (A) Percentage RMS error in estimating the crosstalk-free signal, using either the raw EMG or the output of SOBI or NLSTF. (B) Error in estimating the median frequency.

MDF and MNF errors when using NLSTF were 30.4%, 9.6%, 60.7% and 20.8%, respectively (in the case of SOBI, there were reductions of 25.2% of RMS error and 42.7% in MDF estimation, but MNF was estimated worse); on the other hand, when the force level of the target muscle was equal or larger than that of crosstalk, the median reduction of the reconstruction error by using NLSTF was 20.2% and the differences on RMS amplitude and spectral indexes were very small (median around 3% for the amplitude and 0.03 Hz for the spectral indexes), whereas using SOBI the reconstruction error was reduced of 10.5%, but spectral indexes were estimated worse than using the raw signal.

The same tests were also done for the NLSTF including a third SD channel placed in the mean position between the other two and with same IED. Marginal variations were obtained in the approximation of the target bipolar EMGs: the median RMS errors of filtered data were 17.4% and 16.2% when including 2 or 3 SD signals, respectively, with a median percentage reduction of 5.7%. The estimations of RMS amplitude were fairly similar and spectral indexes had median differences of less than 0.1 Hz.

Concerning experimental data, multifactorial ANOVA tests were employed to investigate the effect of different factors on performance indexes, using the same approach as for simulated data. A paired comparison was studied evaluating differences of performance indexes on same conditions. Specifically, the differences of RMS errors and of mistakes in MDF estimation were computed when considering signals processed by the NLSTF instead of either the raw data or the output of SOBI. These variables of interest were transformed (preserving ranks) to make the residual error after linear fitting closer to Gaussian and homoscedastic. Table 3 shows indexes measuring the fit of the hypotheses of parametric ANOVA. Such a test was then applied and statistically significant terms were obtained, as reported in table 4. The force levels and the muscle considered as target were the factors most selected as significant in the ANOVA models. The original distributions had large queues (reflected into a great kurtosis, especially in the case of the comparison NLSTF vs SOBI), which were largely reduced by the transformation. Possibly, this is the reason why the factor IED was not significant on transformed data (whereas it was when applying ANOVA test to not-transformed data of MDF estimation).

Figure 5 shows a summary of results obtained from experimental data. The percentage RMS error in approximating the bipolar EMG from the target muscle and the absolute error in estimating its MDF are given in figures 5(A) and (B), respectively. The results were pooled showing single effects. As in the case of the tests in simulations, the effect of crosstalk increases when using a larger IED (as the filter is less selective in that case). We also note that the PT is more affected by crosstalk from FCR than vice versa (this clear outcome is also supported by ANOVA results in table 4). SOBI shows some problems in identifying FCR, as the error in estimating the signal from the target muscle is even worse than using

Table 3. Same as table 1, but considering experimental data.

	NLSTF—Raw					
	RMS error			Error in MDF estimation		
	Raw data	Box-Cox $\lambda = 5.04$	Monotone Transform	Raw data	Box-Cox $\lambda = 3.22$	Monotone Transform
Goodness of fit	0.89	0.93	0.08	0.93	0.88	0.05
Skewness	−1.91	−0.61	0.01	−2.42	−0.44	−0.01
Kurtosis	10.82	3.80	3.18	15.00	4.73	2.88
CoV(σ)	1.00	0.62	0.31	0.77	0.54	0.33
	NLSTF—SOBI					
	RMS error			Error in MDF estimation		
	Raw data	Box-Cox $\lambda = 8.44$	Monotone Transform	Raw data	Box-Cox $\lambda = 5.16$	Monotone Transform
Goodness of fit	1.30	0.82	0.05	1.24	0.84	0.09
Skewness	−5.37	−3.04	0.005	−4.84	−4.39	−0.001
Kurtosis	45.08	12.84	2.85	26.11	22.60	2.62
CoV(σ)	1.50	0.96	0.27	1.56	1.20	0.21

Table 4. Same as table 2, but for experimental data.

		Experiments—significant terms in ANOVA model ($p < 0.01$)
NLSTF—Raw	RMS error	Target muscle, force (M1 and M2).
	MDF error	Target muscle, force (M1 and M2), target muscle-force M1.
NLSTF—SOBI	RMS error	Target muscle, force (M1 and M2), target muscle-force M2.
	MDF error	Target muscle-force (M1 and M2).

raw data. Moreover, spectral indexes measured from the output of SOBI are statistically worse than using raw data. As expected, the relative contribution of crosstalk decreases as the force of the target muscle increases; moreover, it increases with the force level of the crosstalk muscle (the same is found for simulations; results are not shown, but average outcomes are given in the text). In fact, statistically significant effects of the force levels are disclosed by ANOVA tests (table 4).

Considering the entire dataset, the following median RMS errors were obtained, when estimating the target SD signal using raw data, SOBI and NLSTF, respectively: 58.1%, 59.4% and 44.1% (there was an improvement over raw data only when using the NLSTF, with median 11.3%, median percentage reduction of the error equal to 19.4%). The error in RMS amplitude estimation was about 20.0% with raw data and 8.4% when using the NLSTF (with a median improvement of 6.8% and a median percentage reduction of the error of 33.8%). Clear improvements in the estimation of spectral indexes were found only when using NLSTF: the error in estimating MDF when using raw data or NLSTF were 2.50 Hz and 1.58 Hz (median difference 0.60 Hz, median percentage reduction 24.2%); the error in estimating MNF when using raw data or NLSTF were 2.46 Hz and 1.69 Hz (median difference 0.42 Hz, median percentage reduction 17.2%).

Additional tests checked the usefulness in the design of the NLSTF of the inclusion of a third SD channel placed between the investigated muscles (at the mean position between the other two channels and with same IED). Marginal improvements were obtained in the approximation of the target bipolar EMGs: the median RMS error of filtered data was 45.6% and 44.8% when including 2 or 3 SD signals, respectively, with a median percentage reduction of 0.7% (as reference, the median RMS of raw data is 58.1%, as indicated above; the median variations in the estimations of median and mean frequencies were below 0.1 Hz).

4. Discussion

Due to the large detection volume, a surface EMG channel placed over a target muscle of interest records also an undesired crosstalk signal produced by the contraction of adjacent muscles [8, 9, 35, 47]. Different advanced methods have been proposed to attenuate crosstalk [20, 26, 28, 30, 37, 47], but using simple spatial filters is still the most used approach in many fields [17, 19].

However, the selectivity of spatial filters depends on tissue properties [12] and the detection volume is reduced so that only a small portion of the target muscle is explored, posing a problem of representativeness of the activity of the entire muscle [27]. To

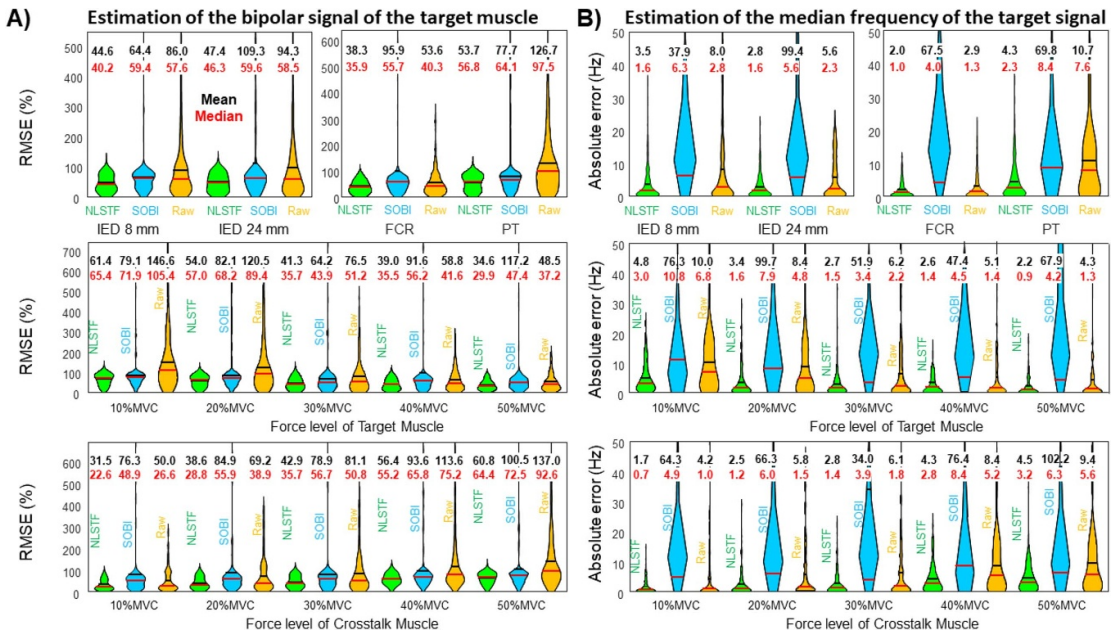

Figure 5. Summary of results from the experimental data, which were pooled to show different parameters of interest: IED of 8 mm or 24 mm, target muscle either flexor carpi radialis (FCR) or pronator teres (PT), different contraction levels of either the target or the crosstalk muscle. Violin plots are shown with indication of median and mean of the distributions. (A) Percentage RMS error in estimating the crosstalk-free signal, using either the raw EMG or the output of SOBI or NLSTF. (B) Error in estimating the median frequency.

overcome these limitations, the OSTF was developed to adapt to the anatomy of the subject and discard crosstalk, while keeping the maximal energy of the contribution from the target muscle [35]. However, the OSTF produces different outputs when applied to different data, so that the possibility of comparing different conditions is limited.

An ideal solution to crosstalk would allow to record the crosstalk-free EMG from the target muscle in a standard filter configuration. Bipolar EMGs are very popular, as they are easy to use and interpret, they require small resources of memory and power, they minimally restrain movements, they can have a large detection volume (if IED is not too small) guaranteeing to record much information from the target muscle and have been applied in many fields (e.g. ergonomics [31], sport science [32], gait analysis [33] and clinics [34]). Thus, in this paper a nonlinear spatio-temporal filter (NLSTF) is introduced to estimate the crosstalk-free bipolar EMG from a target muscle of interest, combining information from few channels recording from target and crosstalk muscles. The new filter is compared to using simply the raw data or applying SOBI approach in the same conditions (i.e. identifying the de-mixing matrix on training data and applying it to the test data to recover the target, thus using a spatial filter adapted to the data).

Both simulated (figure 1) and experimental data (figure 2) have been included to test the performances of the NLSTF. Various conditions are considered, including different IEDs of the bipolar signals, locations of the detection point (at different distances from the crosstalk muscle), anatomies (i.e. different subjects in the experiments and different simulated fat layer thicknesses), and detection problems (simulations of myoelectric fatigue in test data, not-selective conditions in training data, noisy EMGs). The proposed filter is able to reduce the effect of crosstalk, offering the possibility to better investigate the EMG from the target muscle and to decrease the bias in parameter estimation (e.g. amplitude and spectral indexes). Some representative examples are shown in figure 3: the perturbation introduced by crosstalk is evident (for both simulated and experimental EMGs), both in time and frequency domain. Overall results are finally shown in figure 4 (simulated data) and figure 5 (experiments). The effects of different parameters are in line with our expectations, with larger effects of crosstalk in case of less selective conditions. The NLSTF cuts-off the errors in estimating the signal from the target muscle by about 20% in the average (both in simulated and experimental signals).

Moreover, the NLSTF allows more reliable measurements of the RMS amplitude (marginal effect on simulated data, about 34% reduction of the error on experimental data) and of spectral indexes MDF and MNF (average reduction of the error of more than 40% for the simulated signals and about 20% for the experimental data). SOBI shows worse performances, especially in estimating spectral indexes.

In tests on experimental data, a decrease of performance was noted, especially when considering PT as target muscle, which is also the case in which the level of crosstalk is larger. Possibly, it was hard to get

selective contractions of the two investigated muscles. Indeed, SOBI showed great problems in processing experimental data, possibly because the hypothesis of de-correlation of the sources was not met, due to the not selective contractions. In simulations, the addition of a small contribution from the crosstalk muscle on training data did not compromise performances, but it is possible that in experiments the importance of the problem was much greater.

In addition, crosstalk-free signals were available in simulations, whereas they were not in experimental data, where the possible co-contraction of the crosstalk muscle could not be revealed. Thus, if the target signal to be estimated was affected by crosstalk induced by an unwanted contraction of the other muscle, this would reasonably make a major contribution to the estimation error (and this would be true even if the estimates were ideal).

Moreover, other problems may affect experimental data: for example, the possibility that other non investigated nearby muscles contribute to crosstalk and the misalignment of the detection channels (having parallel distributions of electrodes) with the fibres of the two muscles (which can be not perfectly parallel and can also move during the investigated contractions).

These problems were sometimes evident from the inspection of the data from the high-density electrode grid (including 5 parallel arrays of electrodes). Indeed, in some subjects and during some contractions, there were problems among the followings: misalignment of the fibres with respect to the electrodes, their different orientations across the two muscles, different locations of the IZs, lack of selectivity. Careful selection of the best electrodes could have improved the results, but was not implemented in this study, where the most distal portion of the electrode grid was always used: in this way, an experimental condition was mimicked in which electrode placement is guided only by prior visual inspection and palpation of the muscles of interest.

However, even considering the above technical problems and limitations, the advantage of applying the NLSTF was evident in all conditions, even in the worst cases.

In particular, the performances of NLSTF were always superior to those of SOBI. The latter, as well as other BSS methods, is only based on a statistical assumption (i.e. de-correlation of sources for SOBI, independence for other BSS approaches), along with an underlying mixture model. Thus, the output is not forced to approximate the bipolar data from each muscle (as a difference with respect to NLSTF), but eventually they are retrieved if the assumption on sources is satisfied. However, inter-muscular coupling can arise and affect the hypothesis of de-correlation of sources [48, 49]. Moreover, SOBI assumes a linear instantaneous mixture model, so that the de-mixing matrix applies a simple spatial filter. A convolutive model would allow to include also temporal filters, but the training would require more data (indeed, the statistical hypothesis is quite weak, with respect to the one used to build the NLSTF, which forces its output to be the target signal of interest). However, still a linear processing would be applied to the data, even using a convolutive mixture model. The proposed NLSTF improves the flexibility of the processing algorithm by including also quadratic terms (thus, energetic components and cross-correlation) among the predictors used to estimate the target signal. In summary, the stronger constraint imposed by the optimization problem (i.e. fitting the target signal of interest instead of requiring a statistical property of sources), the inclusion of delayed data (and thus the possibility of making also a temporal filter, not only a spatial one) and the nonlinear processing are the key features that probably justify the superior performance of NLSTF over SOBI.

The application of the NLSTF has a very small computational cost. In fact, in the test phase the application of the filter requires only making some algebraic manipulations of the data. The time needed to process epochs of duration 4 s (a subset of 1000 tests was considered) took 14.7 ± 2.3 ms (mean $\pm$ std; i.e. in the average, about the 0.4% of the duration of the processed epoch), using an interpreted single core implementation in MATLAB on a PC with average performances (with Intel Core i7-2630QM, Quad-Core, clock frequency of 2 GHz, 6 GB of RAM, and 64-bit operating system). Implementing the method in a low level programming software and using a compiled version can further reduce the computational time, if needed.

The NLSTF is assumed to be able to recognize the filtering effect of the volume conductor, which transfers the signal from the MU sources of the crosstalk muscle to the detection channel placed over the target muscle. However, the volume conductor filtering depends on the location of the source and of the detection point [50, 51]. For example, different components of the MUAPs (namely, the propagating and the non-propagating components) decay differently depending on the relative distance between the source and the detection point [25, 50]. Moreover, details of tissue geometry and conductivity influence the specific volume conductor filtering and, as a consequence, the shapes of the recorded MUAPs [50]. As the crosstalk muscle is constituted by different MUs located in different positions, the recorded signal is the result of different contributions, generated by sources filtered in different ways by the volume conductor. Thus, a filter which attenuates optimally all their contributions does not exist. Therefore, we can expect that the estimated NLSTF is a compromise among the need of attenuating all MUAPs from the crosstalk muscle. The activity of different sources will contribute to the definition of the NLSTF depending on their amplitude (relying on the size and proximity

of each MU to the detection channel) and their effective activity in the training signal (i.e. a MU which is active and fires a lot will be more represented in the training signal and will have a larger weight in defining the NLSTF with respect to another with MUAP of similar amplitude which has a lower firing frequency in the training signal). In order to give the correct balance to the different sources, it is useful that the training data include about the same contributions as the test set. The specific timings of the MU firings is not a great concern, as is the progressive decrease of CV induced by muscle fatigue: as far as the filtering effect of the volume conductor on the MU sources is well recognized, the NLSTF is expected to maintain its performances (as confirmed by figure 4). On the other hand, some problems are expected in dynamic contractions, in which the volume conductor and the relative positions of the sources and detection channels change. In addition, questions and concerns may arise about long-term use of the filter, as slow drifts (e.g. due to drying of the electrode gel, subject sweat, or relative displacement of muscles and electrodes, or increase in contact impedance) could induce changes that would require recalibration. The investigation of these conditions is beyond the aims of the present work and left for future study.

An additional perspective is the extension to a high-density recording system. Estimating the crosstalk-free signal of each channel over the target muscle is straightforward: more predictors could be included in the matrix X defined in equation (2). Some preliminary tests of the beneficial effect of adding more information from other channels have been performed including a third bipolar detection placed over the mid-line separating the two muscles, obtaining a small (even if statistically significant, according to Wilcoxon signed rank test) improvement (in the average, the estimation error was reduced of 5.7% and 0.7% in simulated and experimental conditions, respectively).

If more detection channels are recorded, other important information could be extracted, e.g. muscle fibre CV. The investigation of this point is left to future studies: it requires experimental tests with more signals recorded from channels aligned to the muscle fibres (two separate linear arrays of electrodes are suggested, to better align with the fibres of the two muscles studied, as in [20]).

The same method could be applied to estimate other crosstalk-free signals, as those provided by monopolar or double differential filters. This is a further interesting extension of this study that can be investigated in the future.

5. Conclusion

An innovative NLSTF is introduced to estimate a bipolar EMG signal cleaned of crosstalk. The method requires a training phase, based on selective data recorded from the target and crosstalk muscles, in order to adapt to the volume conductor and specific conditions. The NLSTF has shown clear advantages in retrieving information from the target muscle compared to the use of raw EMG or the processing by a blind source separation approach. The method is proposed here to support applications in which single bipolar channels are placed over different muscles of interest (common methodology in applied fields like ergonomics, sport science or clinics). Extensions concerning different spatial filters estimation or in high-density surface EMG recordings are interesting future prospects.

Data availability statement

The data cannot be made publicly available upon publication because they are owned by a third party and the terms of use prevent public distribution. The data that support the findings of this study are available upon reasonable request from the authors.

Acknowledgments

Experimental data were recorded by Dr M Raggi of the Mathematical Biology and Physiology research group (Department of Electronics and Telecommunications, Politecnico di Torino, Turin, Italy), under the supervision of Prof. G Boccia of the NeuroMuscularFunction research group (Department of Clinical and Biological Sciences, University of Torino, Turin, Italy).

Funding

This research received no external funding.

Ethical approval

The study was approved by the Ethical Committee of University of Torino (Approval No: 510190) and all participants gave informed consent before starting the study.

Conflicts of interest

The author declares no conflict of interest.

ORCID iD

Luca Mesin https://orcid.org/0000-0002-8239-2348

References

[1] Naik G, Kumar D and Palaniswami M 2014 Signal processing evaluation of myoelectric sensor placement in low-level gestures: sensitivity analysis using independent component analysis *Expert Syst.* **31** 91–99

[2] Besomi M *et al* 2019 Consensus for experimental design in electromyography (CEDE) project: electrode selection matrix *J. Electromyogr. Kinesiol.* **48** 128–44
[3] Péter A, Andersson E, Hegyi A, Finni T, Tarassova O, Cronin N, Grundström H and Arndt A 2019 Comparing surface and fine-wire electromyography activity of lower leg muscles at different walking speeds *Front. Physiol.* **10** 1283
[4] Merlo A, Bó M C and Campanini I 2021 Electrode size and placement for surface EMG bipolar detection from the brachioradialis muscle: a scoping review *Sensors* **21** 7322
[5] Campanini I, Merlo A, Disselhorst-Klug C, Mesin L, Muceli S and Merletti R 2022 Fundamental concepts of bipolar and high-density surface EMG understanding and teaching for clinical, occupational and sport applications: origin, detection and main errors *Sensors* **22** 4150
[6] Talib I, Sundaraj K, Lam C K, Hussain J and Ali M A 2019 A review on crosstalk in myographic signals *Eur. J. Appl. Physiol.* **119** 9–28
[7] Mitchell Barr K, Miller A L and Chapin K B 2010 Surface electromyography does not accurately reflect rectus femoris activity during gait: impact of speed and crouch on vasti-to-rectus crosstalk *Gait Posture* **32** 363–8
[8] Hug F 2011 Can muscle coordination be precisely studied by surface electromyography? *J. Electromyogr. Kinesiol.* **21** 1–12
[9] Jiang N, Englehart K B and Parker P A 2009 Extracting simultaneous and proportional neural control information for multiple-DOF prostheses from the surface electromyographic signal *IEEE Trans. Biomed. Eng.* **56** 1070–80
[10] Ison M and Artemiadis P 2014 The role of muscle synergies in myoelectric control: trends and challenges for simultaneous multifunction control *J. Neural Eng.* **11** 051001
[11] Zhao N, Zhao B, Shen G, Jiang C, Wang Z, Lin Z, Zhou L and Liu J 2023 A robust HD-sEMG sensor suitable for convenient acquisition of muscle activity in clinical post-stroke dysphagia *J. Neural Eng.* **20** 016018
[12] Mesin L, Smith S, Hugo S, Viljoen S and Hanekom T 2009 Effect of spatial filtering on crosstalk reduction in surface EMG recordings *Med. Eng. Phys.* **31** 374–83
[13] Stoykov N S, Lowery M M and Kuiken T A 2005 A finite-element analysis of the effect of muscle insulation and shielding on the surface EMG signal *IEEE Trans. Biomed. Eng.* **52** 117–21
[14] Mesin L 2008 Simulation of surface EMG signals for a multilayer volume conductor with a superficial bone or blood vessel *IEEE Trans. Biomed. Eng.* **55** 1647–57
[15] Lowery M M, Stoykov N S, Taflove A and Kuiken T A 2002 A multiple-layer finite-element model of the surface EMG signal *IEEE Trans. Biomed. Eng.* **49** 446–54
[16] Lowery M M, Stoykov N S, Dewald J P A and Kuiken T A 2004 Volume conduction in an anatomically based surface EMG model *IEEE Trans. Biomed. Eng.* **51** 2138–47
[17] De Luca C J, Kuznetsov M, Gilmore L and Roy S 2011 Inter-electrode spacing of surface EMG sensors: reduction of crosstalk contamination during voluntary contractions *J. Biomech.* **45** 555–61
[18] Solomonow M, Baratta R, Bernardi M, Zhou B, Lu Y, Zhu M and Acierno S 1994 Surface and wire EMG crosstalk in neighbouring muscles *J. Electromyogr. Kinesiol.* **4** 131–42
[19] Farina D, Arendt-Nielsen L, Merletti R, Indino B and Graven-Nielsen T 2003 Selectivity of spatial filters for surface EMG detection from the tibialis anterior muscle *IEEE Trans. Biomed. Eng.* **50** 354–64
[20] Farina D, Fevotte C, Doncarli C and Merletti R 2004 Blind separation of linear instantaneous mixtures of nonstationary surface myoelectric signals *IEEE Trans. Biomed. Eng.* **51** 1555–67
[21] Merletti R, De Luca C J and Sathyan D 1994 Electrically evoked myoelectric signals in back muscles: effect of side dominance *J. Appl. Physiol.* **77** 2104–14
[22] Lowery M, Stoykov N and Kuiken T 2003 A simulation study to examine the use of cross-correlation as an estimate of surface EMG cross talk *J. Appl. Physiol.* **94** 1324–34
[23] Dimitrova N A, Dimitrov G V and Nikitin O A 2002 Neither high-pass filtering nor mathematical differentiation of the EMG signals can considerably reduce cross-talk *J. Electromyogr. Kinesiol.* **12** 235–46
[24] Campanini I, Merlo A, Degola P, Merletti R, Vezzosi G and Farina D 2007 Effect of electrode location on EMG signal envelope in leg muscles during gait *J. Electromyogr. Kinesiol.* **17** 515–26
[25] Mesin L 2019 Separation of interference surface electromyogram into propagating and non-propagating components *Biomed. Signal Process. Control* **52** 238–47
[26] Mesin L 2020 Inverse modelling to reduce crosstalk in high density surface electromyogram *Med. Eng. Phys.* **85** 55–62
[27] Vieira T M, Botter A, Muceli S and Farina D 2017 Specificity of surface EMG recordings for gastrocnemius during upright standing *Sci. Rep.* **7** 13300
[28] Germer C, Farina D, Elias L, Nuccio S, Hug F and Del Vecchio A 2021 Surface EMG crosstalk quantified at the motor unit population level for muscles of the hand, thigh and calf *J. Appl. Physiol.* **131** 808–20
[29] Chen C, Yu Y, Sheng X, Farina D and Zhu X 2021 Simultaneous and proportional control of wrist and hand movements by decoding motor unit discharges in real time *J. Neural Eng.* **18** 056010
[30] Mesin L 2015 Real time identification of active regions in muscles from high density surface electromyogram *Comput. Biol. Med.* **56** 37–50
[31] Gazzoni M, Afsharipour B and Merletti R 2016 Surface EMG in ergonomics and occupational medicine *Surface Electromyography: Physiology, Engineering and Applications* vol 31 (Wiley) pp 361–91
[32] Vigotsky A D, Halperin I, Lehman G J, Trajano G S and Vieira T M 2018 Interpreting signal amplitudes in surface electromyography studies in sport and rehabilitation sciences *Front. Physiol.* **8** 985
[33] Papagiannis G I, Triantafyllou A I, Roumpelakis I M, Zampeli F, Garyfallia Eleni P, Koulouvaris P, Papadopoulos E C, Papagelopoulos P J and Babis G C 2019 Methodology of surface electromyography in gait analysis: review of the literature *J. Med. Eng. Technol.* **43** 59–65
[34] Campanini I, Disselhorst-Klug C, Rymer W Z and Merletti R 2020 Surface EMG in clinical assessment and neurorehabilitation: barriers limiting its use *Front. Neurol.* **11** 934
[35] Mesin L 2018 Optimal spatio-temporal filter for the reduction of crosstalk in surface electromyogram *J. Neural Eng.* **15** 016013
[36] Raggi M, Boccia G and Mesin L 2023 Reduction of crosstalk in the electromyogram: experimental validation of the optimal spatio-temporal filter *IEEE Access* **11** 112075–84
[37] Magbonde A, Quaine F and Rivet B 2022 Comparison of blind source separation methods to surface electromyogram for extensor muscles of the index and little fingers *2022 44th Annual Int. Conf. IEEE Engineering in Medicine & Biology Society (EMBC)* (IEEE) pp 3615–8
[38] Mesin L, Ghani U and Niazi I K 2023 Non-linear adapted spatio-temporal filter for single-trial identification of movement-related cortical potential *Electronics* **12** 1246
[39] Tibshirani R 1996 Regression shrinkage and selection via the lasso *J. R. Stat. Soc.* **58** 267–88
[40] Belouchrani A, Abed-Meraim K, Cardoso J-F and Moulines E 1997 A blind source separation technique using second-order statistics *IEEE Trans. Signal Process.* **45** 434–43
[41] Mesin L, Holobar A and Merletti R 2011 Blind source separation. Application to biomedical signals *Advanced Methods of Biomedical Signal Processing* (*IEEE Press Series in Biomedical Engineering*) ed S Cerutti and C Marchesi (Wiley) ch 15, pp 379–409
[42] Farina D, Mesin L, Martina S and Merletti R 2004 A surface EMG generation model with multilayer cylindrical description of the volume conductor *IEEE Trans. Biomed. Eng.* **51** 415–26

[43] Fuglevand A J, Winter D A and Patla A E 1993 Models of recruitment and rate coding organization in motor-unit pools *J. Neurophysiol.* **70** 2470–88
[44] Andreassen S and Arendt-Nielsen L 1987 Muscle fiber conduction velocity in motor units of the human anterior tibial muscle: a new size principle parameter *J. Physiol.* **391** 561–71
[45] Box G E P and Cox D R 1964 An analysis of transformations *J. R. Stat. Soc.* B **26** 211–52
[46] Hoffmann H 2023 Violin plot (MATLAB Central File Exchange) (available at: www.mathworks.com/matlabcentral/fileexchange/45134-violin-plot)
[47] Mesin L 2020 Crosstalk in surface electromyogram: literature review and some insights *Phys. Eng. Sci. Med.* **43** 481–92
[48] Kilner J M, Baker S N and Lemon R N 2002 A novel algorithm to reduce electrical cross-talk between surface EMG recordings and its application to the measurement of short-term synchronization in humans *J. Physiol.* **538** 919–30
[49] Garcia-Retortillo S and Ivanov P C 2022 Inter-muscular networks of synchronous muscle fiber activation *Front. Netw. Physiol.* **2** 1059793
[50] Mesin L 2013 Volume conductor models in surface electromyography: computational techniques *Comput. Biol. Med.* **43** 942–52
[51] Mesin L 2013 Volume conductor models in surface electromyography: applications to signal interpretation and algorithm test *Comput. Biol. Med.* **43** 953–61